# AN INVESTIGATION OF HYBRID LES/RANS MODELS FOR PREDICTING FLOW FIELDS WITH SEPARATION

**Ken-ichi Abe and Yoshihiro Miyata**
Department of Aeronautics and Astronautics,
Kyushu University
Hakozaki, Higashi-ku, Fukuoka 812-8581, Japan
abe@aero.kyushu-u.ac.jp

## ABSTRACT

A hybrid approach connecting large eddy simulation (LES) with the Reynolds-averaged Navier-Stokes (RANS) modeling in the near-wall region is studied. In contrast to most of the previous studies that have employed linear eddy-viscosity models, in this study, an advanced non-linear eddy-viscosity model is introduced to resolve the near-wall stress anisotropy more correctly. The proposed model is applied to a periodic hill flow with massive separation, as well as fundamental fully-developed plane channel flows. In the calculations, various grid resolutions are used to investigate the model performance in detail. The present model provides encouraging results for further development of this kind of hybrid LES/RANS model.

## INTRODUCTION

Large eddy simulation (LES) is well known as a promising way to predict complex turbulence and turbulent scalar transfer. Although LES needs far fewer grid nodes compared to direct numerical simulation (DNS), there still remains a serious difficulty in its application to high Reynolds-number ($Re$) flows. For instance, reasonable LES for a channel flow needs a grid resolution such as $\Delta x^+ \sim 100$ ($x$: the streamwise direction) and $\Delta z^+ \sim 20$ ($z$: the spanwise direction) in the near-wall region, as well as $\Delta y^+ \sim 1$ in the wall-normal direction, where the no-slip condition is specified at the wall surface. Note that $(\ \ )^+$ denotes a value normalized by the friction velocity $u_\tau$. When LES is applied to the channel flow at $Re_\tau = 10^4$, where $Re_\tau$ $(= u_\tau H/\nu)$ is the Reynolds number based on the half channel height ($H$) and the friction velocity, the aforementioned grid resolution $\Delta z^+ = 20$ means $\Delta z = 2 \times 10^{-3} H$ (i.e., 500 grid points per $H$ in $z$-direction), which is unrealistic for a practical LES. Such being the case, the requirement of the grid resolution for high $Re$ LES is significant.

To overcome this difficulty, a great deal of effort has gone into the development and improvement of the LES model. The key factor is how we can reduce the computational cost in the near-wall region for high $Re$ turbulent flows. One promising approach may be, what is called, the "hybrid LES/RANS model." It is originally based on the concept of a hybrid model connecting LES with Reynolds-averaged Navier-Stokes (RANS) modeling in the near-wall region. So far, a number of research groups have tackled this challenging problem (see for example, Balaras et al. 1996; Nikitin et al. 2000; Hamba 2001; Piomelli et al. 2003; Davidson and Peng 2003; Batten et al. 2004; Hanjalic et al. 2004; Temmerman et al. 2005). Every approach has provided encouraging results and useful knowledge for the development of such a hybrid model.

On the other hand, very few studies have been reported regarding detailed discussion on the near-wall turbulence when hybrid LES/RANS models are applied to flow predictions. The main reason is that most of the previous LES/RANS models have adopted linear eddy-viscosity models (LEVMs), which can never predict the near-wall anisotropy correctly. However, this issue is becoming more important because the RANS model always covers the near-wall region in a hybrid LES/RANS model. This is, naturally, of particular concern in relation to scalar (heat and mass) transfer at walls, in which the turbulence property of the near-wall layer plays a critical role. When an LEVM is used in the near-wall region, any advanced scalar-transfer model based on the generalized gradient-diffusion hypothesis (GGDH, Daly and Harlow 1970) or its higher-order extension (Suga and Abe 2000; Abe and Suga 2001) can never be applied because it needs the correct near-wall limiting behavior of the Reynolds-stress anisotropy. As the first attempt for this purpose, Abe (2005) proposed a hybrid LES/RANS approach with an advanced non-linear eddy-viscosity model (NLEVM) to resolve the near-wall stress anisotropy more correctly.

The present paper is a contribution to the ongoing search for a better hybrid LES/RANS approach applicable to high $Re$ complex turbulence. In this study, the hybrid model by Abe (2005) is applied to a periodic hill flow with massive separation, as well as fundamental fully-developed plane channel flows, with various grid resolutions. By processing the computational results, the present study discusses the model performance in detail.

## TURBULENCE MODELS

### Governing Equations

The filtered (or Reynolds-averaged) governing equations for an incompressible turbulent flow may be written as

$$\partial_i \overline{U}_i = 0 \tag{1}$$

$$\mathrm{D}_t \overline{U}_i = -(1/\rho)\,\partial_i \overline{P} + \partial_j \left\{ \nu \left( \partial_j \overline{U}_i + \partial_i \overline{U}_j \right) - \tau_{ij} \right\} \tag{2}$$

where $\overline{(\ \ )}$ denotes a filtered value in the LES region or a Reynolds-averaged value in the RANS region, respectively. In Eq. (2), $\rho$, $\overline{P}$, $\overline{U}_i$ and $\nu$ respectively denote density, filtered static pressure, filtered velocity and kinematic viscosity. The sub-grid scale (SGS) stress $\tau_{ij}$ is originally expressed as $\tau_{ij} = \overline{U_i U_j} - \overline{U}_i \overline{U}_j$. Note that $\tau_{ij}$ coincides with the general expression for the Reynolds-stress tensor in the RANS region, $\tau_{ij} = \overline{u_i u_j}$, where $u_i$ is defined as $u_i = U_i - \overline{U}_i$.

**NLEVM in the RANS Region**

In order to improve the prediction accuracy in the near-wall region, an anisotropy-resolving algebraic turbulence model is introduced in this study. The Reynolds stress $\overline{u_i u_j}$ in the RANS region is modeled as follows (Abe et al. 2003; Abe 2005):

$$\begin{aligned}\overline{u_i u_j} = 2k\delta_{ij}/3 - 2k\tau C_B \left[1 + \{1 - f_w(26)\} f_{s1}\right] S_{ij} \\ + 4k\tau^2 C_D C_B \{1 - f_w(26)\} \Big\{ - \left(S_{ik}\Omega_{kj} - \Omega_{ik}S_{kj}\right) \\ + (1 - f_{s2}) \left(S_{ik}S_{kj} - S^2\delta_{ij}/3\right) \Big\} + 2k\, {}^w b_{ij} \end{aligned} \quad (3)$$

where $k(= \overline{u_i u_i}/2)$ is the turbulence energy. In Eq. (3), $S_{ij}$ and $\Omega_{ij}$ respectively denote the strain-rate tensor and the vorticity tensor as

$$S_{ij} = \left(\partial_j \overline{U}_i + \partial_i \overline{U}_j\right)/2, \quad \Omega_{ij} = \left(\partial_j \overline{U}_i - \partial_i \overline{U}_j\right)/2 \quad (4)$$

The model function $f_w$ is modeled as follows (Abe et al. 1997):

$$f_w(\xi) = \exp\left\{-(n^*/\xi)^2\right\} \quad (5)$$

where $\xi$ is a prescribed constant. In Eq. (5), $n^*(= (\nu\varepsilon)^{1/4} n/\nu)$ is the non-dimensional wall distance with Kolmogorov scale (Abe et al. 1994), where $\varepsilon$ is the dissipation rate of $k$ and $n$ is uniquely determined as the shortest distance from all the wall surfaces. In the model, the characteristic time scale $\tau$ and the model coefficients are as follows (Abe et al. 2003):

$$\begin{aligned} \tau = \nu_t/k, \quad \nu_t = C_\mu f_\mu k^2/\varepsilon \\ f_\mu = \left[1 + \left(35/R_t^{3/4}\right) \exp\left\{-(R_t/30)^{3/4}\right\}\right] \{1 - f_w(26)\} \\ C_B = \frac{1}{1 + \frac{22}{3}(C_D\tau)^2 \Omega^2 + \frac{2}{3}(C_D\tau)^2 (\Omega^2 - S^2) f_B} \\ f_{s1} = f_{r1} f_{r2} C_{s1} (C_D\tau)^2 \left(\Omega^2 - S^2\right) \\ f_{s2} = f_{r1} f_{r2} \{1 + C_{s2} C_D \tau (\Omega - S)\} \\ f_B = 1 + C_\eta C_D \tau (\Omega - S), \quad f_{r1} = \frac{\Omega^2 - S^2}{\Omega^2 + S^2}, \quad f_{r2} = \frac{S^2}{\Omega^2 + S^2} \\ S^2 = S_{mn}S_{mn}, \quad \Omega^2 = \Omega_{mn}\Omega_{mn}, \quad S = \sqrt{S^2}, \quad \Omega = \sqrt{\Omega^2} \\ C_D = 0.8, \quad C_\mu = 0.12, \quad C_\eta = 100 \\ C_{s1} = 0.15 C_\eta, \quad C_{s2} = 0.07 C_\eta \end{aligned} \quad (6)$$

where $R_t(= k^2/\nu\varepsilon)$ is the turbulent Reynolds number.

In Eq. (3), ${}^w b_{ij}$ is introduced to improve the predictive performance of the near-wall stress anisotropy as follows (Abe et al. 2003):

$$\begin{aligned} {}^w b_{ij} = f_w(26) \Big[ -\alpha_w \frac{1}{2} \left(d_i d_j - \frac{\delta_{ij}}{3} d_k d_k\right) \\ + \left(1 - {f_{r1}}^2\right) {\tau_d}^2 \Big\{ - \frac{\beta_w C_w}{1 + C_w {\tau_d}^2 \sqrt{S^2\Omega^2}} \left(S_{ik}\Omega_{kj} - \Omega_{ik}S_{kj}\right) \\ + \frac{\gamma_w C_w}{1 + C_w {\tau_d}^2 S^2} \left(S_{ik}S_{kj} - \frac{\delta_{ij}}{3} S^2\right) \Big\} \Big] \end{aligned} \quad (7)$$

where

$$\begin{aligned} d_i = N_i/\sqrt{N_k N_k}, \quad N_i = \partial_i n \\ \tau_d = \{1 - f_w(15)\} (k/\varepsilon) + f_w(15)\, \delta_w \sqrt{\nu/\varepsilon} \end{aligned} \quad (8)$$

In this study, the following combined model is used to represent the near-wall fragment:

$$\begin{aligned} {}^w b_{ij} = f_\tau\ {}^{w1} b_{ij} + (1 - f_\tau)\ {}^{w2} b_{ij} \\ f_\tau = \exp\left[-3\{1 - f_w(26)\} (k/\varepsilon) \sqrt{S^2}\right] \\ {}^{w1} b_{ij} = \text{Eq. (7) with } (\alpha_w = 1, \quad \beta_w = 1/4, \quad \gamma_w = 1.5, \\ \delta_w = 1.0, \quad C_w = 0.5) \\ {}^{w2} b_{ij} = \text{Eq. (7) with } (\alpha_w = 0, \quad \beta_w = 13/30, \quad \gamma_w = 0.6, \\ \delta_w = 3.0, \quad C_w = 1.0) \end{aligned} \quad (9)$$

Turbulence energy and its dissipation rate are determined from the usual form of the transport equations:

$$\mathrm{D}_t k = \partial_j \{(\nu + \nu_t/\sigma_k) \partial_j k\} + P_k - \varepsilon \quad (10)$$

$$\mathrm{D}_t \varepsilon = \partial_j \{(\nu + \nu_t/\sigma_\varepsilon) \partial_j \varepsilon\} + C_{\varepsilon 1} (\varepsilon/k) P_k - C_{\varepsilon 2} f_\varepsilon \left(\varepsilon^2/k\right) \quad (11)$$

where $P_k = -\overline{u_i u_j} \partial_j \overline{U}_i$ is the production term of $k$ and

$$\begin{aligned} C_{\varepsilon 1} = 1.45, \quad C_{\varepsilon 2} = 1.83, \quad \sigma_k = 1.2/f_t, \quad \sigma_\varepsilon = 1.5/f_t \\ f_t = 1 + 5.0 f_w(5) \\ f_\varepsilon = \left[1 - 0.3 \exp\left\{-(R_t/6.5)^2\right\}\right] \{1 - f_w(3.3)\} \end{aligned} \quad (12)$$

**SGS Model in the LES Region**

In this study, the model expressions in Eqs. (3) – (8) are also adopted for modeling $\tau_{ij}$ in the LES region (Abe 2005). The turbulence energy $k$ and the dissipation rate $\varepsilon$ in the model expressions are replaced for the SGS values, $k_S$ and $\varepsilon_S$, respectively. In the present model, following the previous studies (Inagaki et al. 2002; Bardina et al. 1980; Horiuti 1993), $k_S$ and $\varepsilon_S$ are modeled as follows:

$$\begin{aligned} k_S = (C_k/2) \left(\overline{U}_i - \widehat{\overline{U}}_i\right)^2, \quad \varepsilon_S = {k_S}^{3/2}/\Delta + 2\nu k_S/n^2, \\ C_k = 4.5, \quad \Delta = (\Delta_x \Delta_y \Delta_z)^{1/3} \end{aligned} \quad (13)$$

where $\widehat{(\ )}$ denotes the filtering operator, for which the Simpson rule is used.

The time scale $\tau$ in Eq. (6) is modeled as follows (Abe and Suga 2001):

$$\tau = C_S \{1 - f_w(26)\} \Delta/\sqrt{k_S}, \quad C_S = 0.12 \quad (14)$$

As for ${}^w b_{ij}$ in Eq. (7), the following model constants are adopted:

$$\begin{aligned} {}^w b_{ij} = \text{Eq. (7) with } (\alpha_w = 0, \quad \beta_w = 13/30, \quad \gamma_w = 0.6, \\ \delta_w = 6.0, \quad C_w = 1.0) \end{aligned} \quad (15)$$

In calculating $\tau_d$ in Eq. (8), $k$ and $\varepsilon$ are simply replaced by $k_S$ and $\varepsilon_S$, respectively.

**The Present Hybrid Approach**

In this study, $\tau_{ij}$ in Eq. (2) is modeled as follows:

$$\tau_{ij} = (1 - f_{hb})\ \overline{u_i u_j}_{(RANS)} + f_{hb}\ \tau_{ij}{}_{(LES)} \quad (16)$$

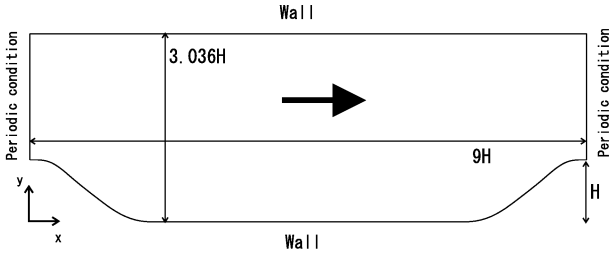


Figure 1: Hill-flow geometry.

where $f_{hb}$ is the model function to connect the LES and RANS regions smoothly. In Eq. (16), $f_{hb}$ is close to 1 in the region away from the wall, where full LES is adopted. On the other hand, the RANS calculation is performed in the near-wall region, where $f_{hb}$ must become close to 0. In this study, the following expression is used for $f_{hb}$:

$$f_{hb} = 1 - \exp\left[-\left\{n/\left(C_{hb}\ \Delta_{||}\right)\right\}^6\right]$$

$$\Delta_{||} = \sqrt{\max\left(\Delta_x\Delta_y, \Delta_y\Delta_z, \Delta_z\Delta_x\right)}, \quad C_{hb} = 4.0 \qquad (17)$$

## TEST CASES AND COMPUTATIONAL CONDITIONS

To investigate the model performance, the aforementioned hybrid LES/RANS model was applied to two flow configurations. The first was a fully-developed plane-channel flow. The Reynolds numbers tested were $Re_\tau = 395$ and 10000, based on friction velocity ($u_\tau$) and the half channel height (H). For the former case, DNS data were reported by Morser et al. (1990). In the calculations, the grid number was 31 ($x$) × 61 ($y$) × 31 ($z$) for both Reynolds numbers. In particular, several grid resolutions ($\Delta_{||}$ =0.1, 0.2, 0.4) were employed at $Re_\tau = 10000$ by changing the domain size ($6H \times 1.5H$, $12H \times 3H$, $24H \times 6H$). Note that the grid resolutions were respectively ${\Delta_{||}}^+$ =1000, 2000 and 4000 in wall unit, while $y^+_{wall} \sim 1$ in the wall-normal direction.

The second test case was a periodic-hill flow illustrated in Fig. 1. The presence of massive separation between consecutive hills allows the model to be investigated for conditions representative of complex separated flows. The Reynolds number was 21200, based on mean velocity ($U_b$) and channel height (3.036H, H: hill height). In the calculations, the spanwise ($z$) width was 4H, while the grid resolution was controlled by changing the grid numbers (61 ($x$) × 61 ($y$) × 31 ($z$), 61 × 61 × 16, 61 × 61 × 9). Note that the grid resolutions in $z$-direction were $\Delta z$ =0.13H, 0.27H and 0.5H, respectively. For this geometry, highly-resolved LES data were reported by Temmerman et al. (2003).

Calculations were performed with the finite-volume procedure STREAM of Lien and Leschziner (1994a), followed by several improvements and substantially upgraded by Apsley and Leschziner (1999). This method uses collocated storage on a grid. The second-order central difference scheme was used for the discretization of each term, except for the convection terms of $k$ (Eq. (10)) and $\varepsilon$ (Eq. (11)) which were discretized by the UMIST scheme (Lien and Leschziner, 1994b), a TVD implementation of the QUICK scheme. The solution algorithm is based on the SIMPLE scheme. As for the time integration, the second-order Crank-Nicolson scheme was employed.

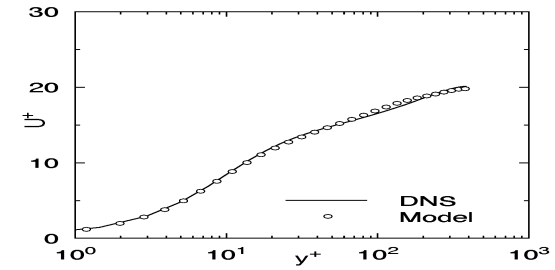


(a) Mean velocity

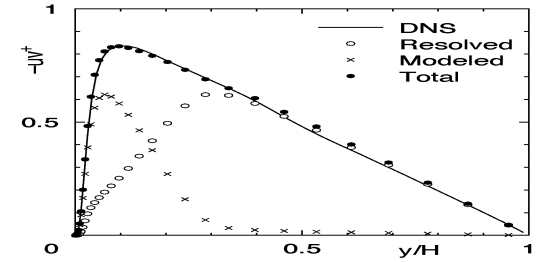


(b) Reynolds shear stress

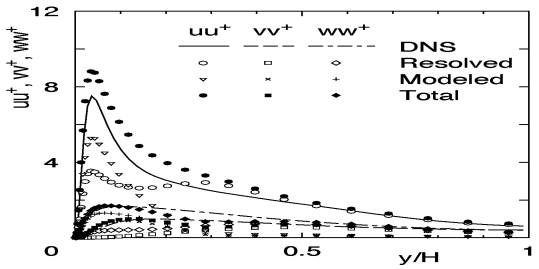


(c) Reynolds normal stresses

Figure 2: Computational results of channel flow ($Re_\tau = 395$, 31 × 61 × 31, 6H × 1.5H, $\Delta_{||} = 0.1H$).

## RESULTS AND DISCUSSION

### Channel-Flow Case

Figure 2 compares the results at $Re_\tau = 395$ for the grid resolution of $\Delta_{||} = 0.1$, corresponding to the flow domain of 6H × 1.5H. As seen in the figures, the predicted profiles of mean velocity and Reynolds-shear stress are smooth and acceptable. Concerning the Reynolds normal stresses, all the components are generally predicted well, though some overestimations are seen for streamwise turbulence. Good performance is obtained in the near-wall (RANS) region, while some suppression of the energy redistribution from the streamwise to the wall-normal and spanwise components is seen in the switching region, resulting in a little stronger stress-anisotropy prediction.

Figures 3 and 4 give the calculated results at $Re_\tau = 10000$. First, the results of the full LES are shown in Fig. 3 with the grid resolution of $\Delta_{||} = 0.05$ (61 × 61 × 61, 6H × 1.5H). The predictions give considerable errors. Although a finer grid resolution is used, typical features of LES with a coarse grid resolution are seen in Fig. 3. This is caused by a very high Reynolds-number condition for the grid resolution used. The mean-velocity profile shows a considerable shift up from the well-known log-law profile. This also means serious underestimation in values of the skin friction coefficient.

On the other hand, as seen in Fig. 4, the present hybrid model provides encouraging results for both the mean veloc-

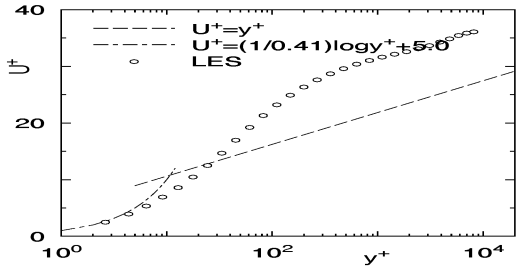


Figure 3: Computational results of full LES ($Re_\tau = 10000$, 61 $\times$ 61 $\times$ 61, 6H $\times$ 1.5H, $\Delta_{||}{}^{+} = 500$).

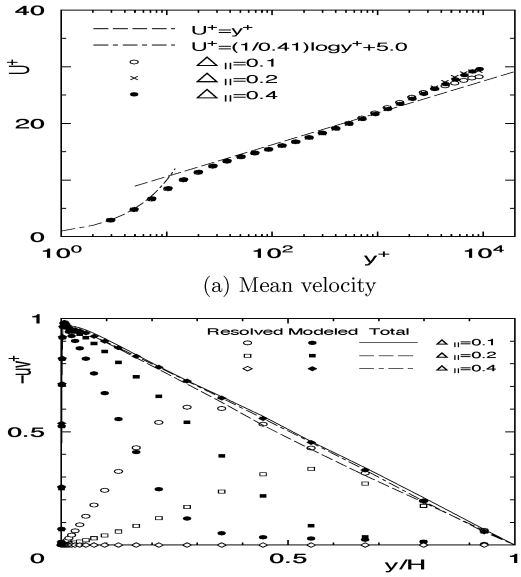


(a) Mean velocity

(b) Reynolds shear stress

Figure 4: Computational results of channel flow ($Re_\tau$ = 10000, 31 $\times$ 61 $\times$ 31).

ity and the Reynolds shear stress, though slight differences are still seen among the velocity profiles with different grid resolutions. In all cases, the mean-velocity profiles are connected smoothly between the LES and RANS regions. It is also understood that the profiles of the total (resolved+modeled) Reynolds shear stress are reasonable and show no conflict with known results.

### Hill-Flow Case

Figure 5 gives overall views, in the form of model-predicted streamfunction plots. In the figure, the results of the present hybrid model with different grid resolutions are compared to those by the highly-resolved LES data by Temmerman et al. (2003). Note that the lines indicating $f_{hb} = 0.5$ are also shown in Figs. 5 (b)–(d) for reference. The reattachment length for the highly-resolved LES data is $4.72H$ (Temmerman et al. 2003), while the hybrid model returns $4.94H$ ($\Delta z = 0.13H$), $5.25H$ ($\Delta z = 0.27H$) and $5.92H$ ($\Delta z = 0.5H$), respectively. Although the present hybrid model generally returns a reasonable separation bubble, some overprediction is seen especially for the case with the grid resolution of $\Delta z = 0.5H$. However, having considered that $0.5H$ is in fact the half hill height (very

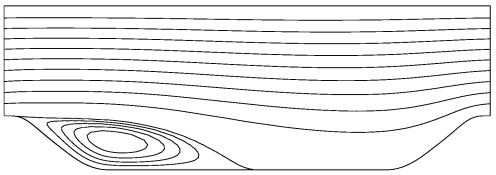

(a) LES (reference)

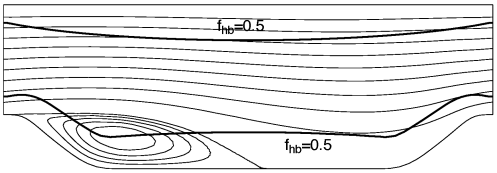


(b) Hybrid (61 $\times$ 61 $\times$ 31, $\Delta z = 0.13H$)

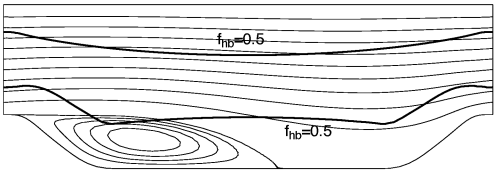


(c) Hybrid (61 $\times$ 61 $\times$ 16, $\Delta z = 0.27H$)

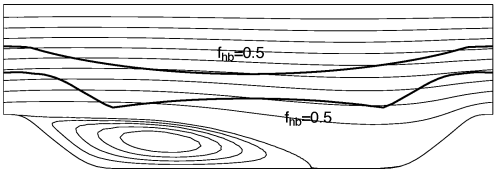


(d) Hybrid (61 $\times$ 61 $\times$ 9, $\Delta z = 0.5H$)

Figure 5: Streamlines of hill flow.

coarse grid resolution), it is thought that the present model performance is encouraging for practical engineering applications.

Figure 6 shows mean-velocity distributions at four streamwise positions, $x/H$ = 2, 4, 6 and 8. The first and second positions are in the recirculation zone, $x/H = 6$ is a short distance behind the reattachment point, while $x/H = 8$ cuts across the windward side of the hill where the flow is subjected to strong acceleration. These four locations may be claimed to represent regions in which several distinctly different types of flow conditions are encountered in the present configuration. As seen in the figure, the present hybrid model generally gives reasonable predictions of the mean velocity. First, in case of $\Delta z = 0.13H$, fairly good agreement is obtained at every location. In case of $\Delta z = 0.27H$, some overestimation is seen in the recirculation region ($x/H = 4$), though the present model still gives reasonable agreement at the other locations. On the other hand, considerable differences are seen in case of $\Delta z = 0.5H$, corresponding to the overestimation of the reattachment length, as was described before.

Figure 7 compares distributions of the predicted total (resolved+modeled) Reynolds shear stress. Although the present hybrid model generally gives reasonable predictions, a considerable underprediction is seen at $x/H = 2$ in case of $\Delta z = 0.5H$. On the other hand, at $x/H = 4$ in case of $\Delta z = 0.13H$, the predicted maximum shear stress is higher than that of the LES by Temmerman et al. (2003), though mean-velocity

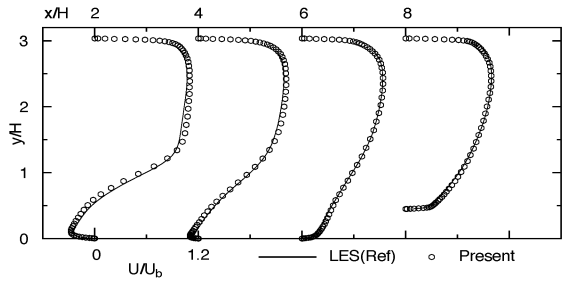


(a) Hybrid ($61 \times 61 \times 31$, $\Delta z = 0.13H$)

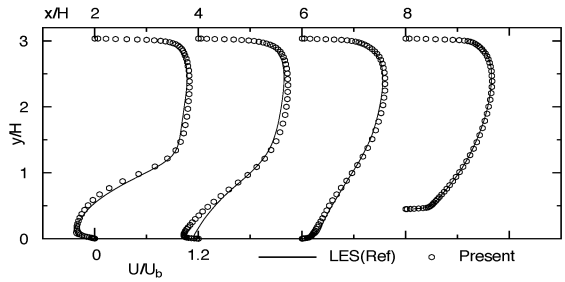


(b) Hybrid ($61 \times 61 \times 16$, $\Delta z = 0.27H$)

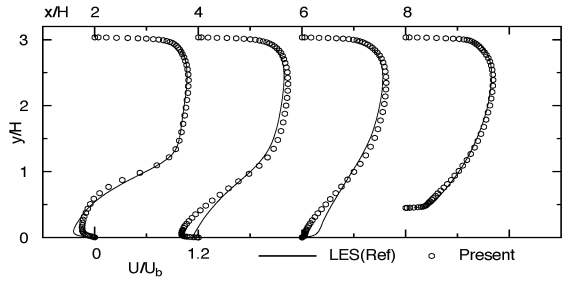


(c) Hybrid ($61 \times 61 \times 9$, $\Delta z = 0.5H$)

Figure 6: Mean-velocity profiles of hill flow.

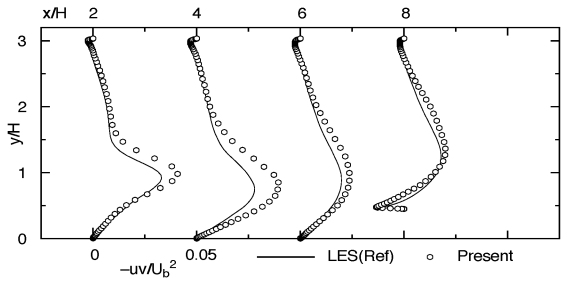


(a) Hybrid ($61 \times 61 \times 31$, $\Delta z = 0.13H$)

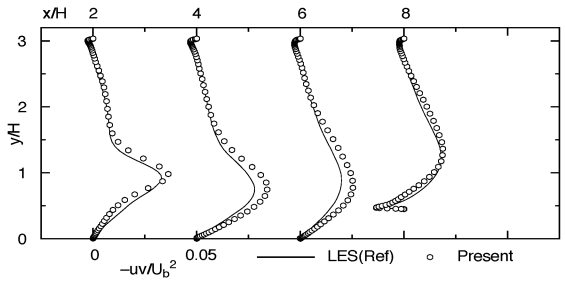


(b) Hybrid ($61 \times 61 \times 16$, $\Delta z = 0.27H$)

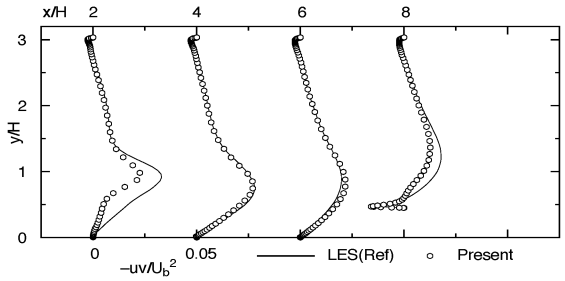


(c) Hybrid ($61 \times 61 \times 9$, $\Delta z = 0.5H$)

Figure 7: Reynolds shear stress profiles of hill flow.

profile shows good agreement. Generally, the Reynolds shear stress would be expected to go hand-in-hand with the prediction accuracy of shear strain (i.e., mean-velocity profile). However, this link ignores the influence of the pressure gradient in the momentum balance, and thus it is not always possible to uniquely relate the two, except for a special case such as a fully-developed channel flow. As seen in the figure, it may be possible that the present results tend to give some overestimations of the Reynolds shear stress compared to the LES by Temmerman et al. (2003), mainly caused by far fewer grid nodes used in the calculations.

The streamwise and wall-normal components of the Reynolds normal stresses are compared with the highly-resolved LES data in Fig. 8. The present model returns reasonable trend of the stress anisotropy, though quantitative agreement is insufficient even for the finest grid-resolution case ($\Delta z = 0.13H$). As mentioned before, however, the present calculation used far fewer grid nodes. For example, the number of grid nodes for the case of $\Delta z = 0.13H$ was about $1.2 \times 10^5$, while $4.6 \times 10^6$ nodes were used for the LES by Temmerman et al. (2003)). Having considered this fact, it is said that the present hybrid model is promising from the engineering viewpoint.

## CONCLUDING REMARKS

A hybrid approach connecting LES with the RANS modeling in the near-wall region was studied. In contrast to most of the previous studies that employed linear eddy-viscosity models, the present model adopts an advanced non-linear eddy-viscosity model (NLEVM) to resolve the near-wall stress anisotropy more correctly. The model was applied to a periodic hill flow with massive separation, as well as fundamental fully-developed plane channel flows, with various grid resolutions. The main conclusions derived from this study are as follows:

- It has been confirmed that the introduction of an anisotropy-resolving NLEVM is very effective in improving the accuracy of the total (resolved+modeled) Reynolds stresses predicted in the near-wall region.
- The present hybrid LES/RANS model gives reasonable mean-velocity profiles and skin-friction coefficients for a high $Re$ channel-flow case at $Re_\tau = 10^4$ ($Re_b \sim 5 \times 10^5$).
- The present hybrid LES/RANS model generally performs well in a periodic hill flow with massive separation, though some errors are still seen in cases with coarser grid resolutions.

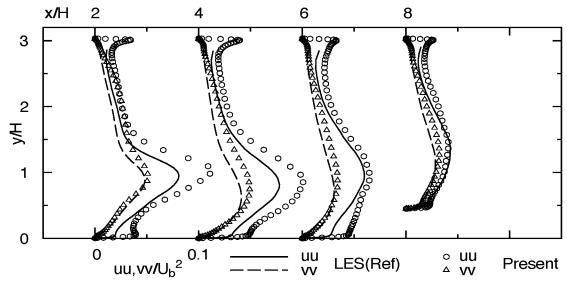


(a) Hybrid ($61 \times 61 \times 31$, $\Delta z = 0.13H$)

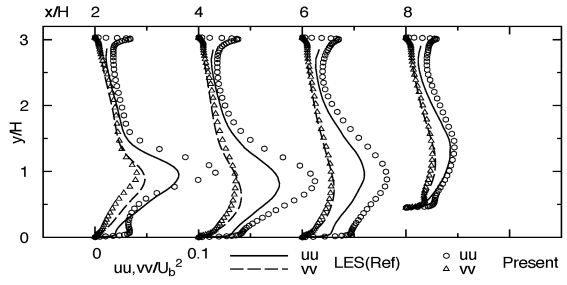


(b) Hybrid ($61 \times 61 \times 16$, $\Delta z = 0.27H$)

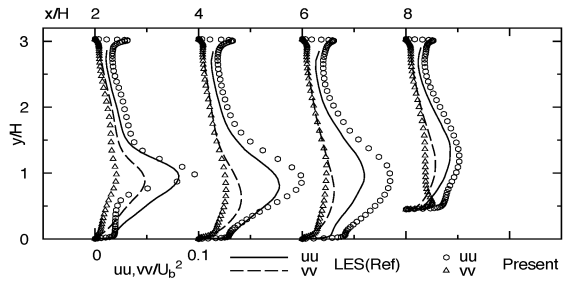


(c) Hybrid ($61 \times 61 \times 9$, $\Delta z = 0.5H$)

Figure 8: Reynolds normal stress profiles of hill flow.

## ACKNOWLEDGEMENTS

This research was partially supported by Grant-in-Aids for Scientific Research, No.15360450, No.15106013, sponsored by the Ministry of Education, Culture, Sports, Science and Technology, Japan. The author wishes to express his appreciation to Professor M.A. Leschziner of Imperial College of Science, Technology and Medicine (IC), London, UK for the support in using the STREAM code.

## REFERENCES

Abe, K., Kondoh T., and Nagano Y. (1994). A New Turbulence Model for Predicting Fluid Flow and Heat Transfer in Separating and Reattaching Flows - I. Flow Field Calculations. *Int. J. Heat Mass Transfer*, **37**, 139-151.

Abe, K., Kondoh, T., and Nagano, Y. (1997). On Reynolds stress expressions and near-wall scaling parameters for predicting wall and homogeneous turbulent shear flows. *Int. J. Heat Fluid Flow*, **18**, 266-282.

Abe, K., and Suga, K. (2001). Towards the development of a Reynolds-averaged algebraic turbulent scalar-flux model. *Int. J. Heat Fluid Flow*, **22**, 19-29.

Abe, K., Jang, Y.J., and Leschziner, M.A. (2003). An investigation of wall-anisotropy expressions and length-scale equations for non-linear eddy-viscosity models. *Int. J. Heat Fluid Flow*, **24**, 181-198.

Abe, K. (2005). A hybrid LES/RANS approach using an anisotropy-resolving algebraic turbulence model, *Int. J. Heat Fluid Flow*, **26**, 204-222.

Apsley, D.D. and Leschziner, M.A. (1999). Advanced turbulence modelling of separated flow in a diffuser. *Flow, Turbulence and Combustion*, **63**, 81-112.

Batten, P., Goldberg, U., and Chakravarthy, S. (2004). Interfacing statistical turbulence closures with large-eddy simulation. *AIAA J.*, **42**, 485-492.

Balaras, E., Benocci, C., and Piomelli, U. (1996). Two-layer approximate boundary conditions for large-eddy simulations. *AIAA J.*, **34**, 1111-1119.

Bardina, J., Ferziger, J.H., and Reynolds, W.C. (1980). Improved subgrid scale models for large eddy simulation. *AIAA Paper*, **80-1357**.

Daly, B.J., and Harlow, F.H. (1970). Transport equations in turbulence. *Phys. Fluids*, **13**, 2634-2649.

Davidson, L., and Peng, S.H. (2003). Hybrid LES-RANS modelling: a one-equation SGS model combined with a $k$-$\omega$ model for predicting recirculating flows. *Int. J. Numer. Meth. Fluids*, **43**, 1003-1018.

Hanjalic, K, Hadziabdic, M., Temmerman, L., and Leschziner, M.A. (2004). Merging LES and RANS strategies: zonal or seamless coupling? *Direct and Large Eddy Simulation V (R. Friedrich et al. (eds))*, Kluwer Academic Publ., 451-464.

Hamba, F. (2001). An attempt to combine large eddy simulation with the $k$-$\varepsilon$ model in a channel-flow calculation. *Theoret. Comput. Fluid Dynamics*, **14**, 323-336.

Horiuti, K. (1993). A proper velocity scale for modeling subgrid-scale eddy viscosities in large eddy simulation. *Phys. Fluids A*, **5**, 146-157.

Inagaki, M., Kondoh, T., and Nagano, Y. (2002). A mixed-time-scale SGS model with fixed model-parameters for practical LES. In: *Engineering Turbulence Modelling and Experiments - 5*, edited by W. Rodi and N. Fueyo, Mallorca, 257-266.

Lien, F.S., and Leschziner, M.A. (1994a). A general non-orthogonal collocated finite volume algorithm for turbulent flow at all speeds incorporating second-moment turbulence-transport closure, Part 1: Computational implementation. *Comput. Methods Appl. Mech. Engrg*, **114**, 123-148.

Lien, F.S., and Leschziner, M.A. (1994b). Upstream monotonic interpolation for scalar transport with application to complex turbulent flows. *Int. J. Num. Meths. Fluids*, **19**, 527-548.

Moser, R.D., Kim, J., and Mansour, N.N. (1999). Direct numerical simulation of turbulent channel flow up to $Re_\tau$=590. *Phys. Fluids*, **11**, 943-945.

Nikitin, N.V., Nicoud, F., Wasistho, B., Squires, K.D., and Spalart, P.R. (2000). An approach to wall modeling in large-eddy simulations. *Phys. Fluids*, **12**, 1629-1632.

Piomelli, U., Balaras, E., Pasinato, H., Squaires, K.D., and Spalart, P.R. (2003). The inner-outer layer interface in large-eddy simulations with wall-layer models. *Int. J. Heat and Fluid Flow*, **24**, 538-550.

Suga, K., and Abe, K. (2000). Nonlinear eddy viscosity modeling for turbulence and heat transfer near wall and shear-free boundaries. *Int. J. Heat Fluid Flow*, **21**, 37-48.

Temmerman, L., Leschziner, M.A., Mellen, C.P. and Froehlich, J. (2003). Investigation of wall-function approximations and subgrid-scale models in Large Eddy Simulation of separated flow in a channel with streamwise periodic constrictions. *Int. J. Heat and Fluid Flow*, **24**, 157-180.

Temmerman, L., Hadziabdic, M., Leschziner, M.A., and Hanjalic, K. (2005). A hybrid two-layer URANS-LES approach for large eddy simulation at high Reynolds numbers. *Int. J. Heat and Fluid Flow*, **26**, 173-190.